Physical Characterization of Wood and Wood–Polymer Composites: An Update

J. R. WRIGHT and L. J. MATHIAS*

Department of Polymer Science, University of Southern Mississippi, Hattiesburg, Mississippi 39406-0076

SYNOPSIS

New and reliable test methods have been developed, and are under development, for the physical characterization of wood and whole wood–polymer composites (WPC is used in this article to refer to polymer-impregnated whole wood). The methods described here have been designed for smaller samples than are required for most ASTM tests. It should be stressed that, when comparing treated samples to untreated samples in any type of testing, the initial density or specific gravity (density before treatment) of the treated sample should be the same as the untreated control sample. If possible, measurements should be made on a given sample before and after treatment; on a split sample, half should be treated and compared with the untreated half. If there is much variation in density between samples within a group, the effectiveness of the treatment cannot be determined with an acceptable degree of accuracy, since whole wood varies greatly between specimens and density is a major factor contributing to property variability. For example, swelling (due to moisture uptake), modulus, toughness, surface hardness, and compressive strength of wood all increase dramatically with increasing density for both untreated whole wood and WPCs.

Scanning electron microscopy, coupled with x-ray energy analysis, indicated the presence or absence of good interaction between wood components and *in situ* formed polymer. For example, poly(EHMA) (the homopolymer of ethyl α-hydroxymethylacrylate) and wood components were seen to be strongly bonded, and x-ray activation elemental analysis confirmed the presence of poly(EHMA) and its copolymers *within* the wood cell walls. On the other hand, proton spin-lattice relaxation in the rotating frame ($T_{1\rho}$) measurements (by ^{13}C solid-state NMR) for balsa/EHMA WPCs gave two separate sets of relaxation times, one each for unique peaks corresponding to either the polymer or the wood components. It is probable that the region of interaction between poly(EHMA) and the wood component in the balsa/EHMA WPC (the interphase region) is small, as compared to the individual components, and is not observed. This result is consistent with a two-parameter relaxation process for the peak at *ca.* 61 ppm, which includes overlapping peaks for the hydroxymethyl carbons of poly(EHMA) and cellulose.

INTRODUCTION

Physical characterization of wood and whole wood–polymer composites (WPC) involves tests used to define immediate and ultimate properties needed to establish product design and strength criteria. Research evaluations and product development are heavily dependent on the results and validity of these tests. However, a major problem with interpreting the specific results exists in the inherent variability between test specimens. Wood properties are so variable in nature that care must be taken not to place too much significance on, or draw a firm conclusion from, only one or a few tests. A particular physical property measurement of one specimen can be significantly different from that of another specimen of the same wood species, and even from the same tree. The coefficient of variation (standard deviation divided by the mean $\times 100$), for measurement of different physical properties within a carefully

* To whom correspondence should be addressed.

Journal of Applied Polymer Science, Vol. 48, 2225–2239 (1993)
 CCC 0021-8995/93/122225-15

selected set of samples from a given tree species, has been shown to range from 10% to 38%.[1] A major factor contributing to this imprecision in measured properties is the density variation of the individual specimens. This article deals with a new interpretation of old tests and the development of new and reliable test methods for smaller samples than are usually required for ASTM tests. Discussion focuses on decreasing the variability between test specimens and improving the validity of the analyses.

WOOD–WATER RELATIONSHIP

Wood is a porous, hygroscopic material, filled with open passageways (lumens), and composed of polymers possessing an abundance of hydroxyl groups in the cell wall structural components. These groups attract water molecules through hydrogen bonding and are in equilibrium with the partial vapor pressure of moisture in the surrounding atmosphere. As the atmospheric and wood moisture content increase, the cell wall swells and the wood expands in direct proportion to the moisture sorbed, until the cell wall is saturated (fiber saturation point). This process is reversible and the wood shrinks as it loses moisture below the fiber saturation point. The total amount of swelling that occurs in whole wood, due to moisture uptake, is directly dependent on the wood density,[2] with the percent volumetric swelling (V) given by

$$V = K_f d \times 100 \qquad (1)$$

where K_f (cm^3/g) is the water content at the fiber saturation point and d (g/cm^3) is the dry wood density. The cellulose content of wood is normally 55–65% crystalline, and this component is not normally accessible to water. Moisture uptake occurs in the amorphous cellulose regions of the wood cell wall, and in the hemicellulose and (to a lesser degree) lignin domains.

One of the most important roles played by the chemical modification of wood and the formulation of wood–polymer composites is in reducing the swelling by water. Cyclic dimensional changes, caused by humidity swings or direct contact with water, lead to rapid debonding, delamination, and loss of structural integrity in whole wood or composites containing particulate wood or fiber. Quantitation of these effects is important. While the test discussed below is not new, the correlations are, and they relate directly to the new characterization methods described in the rest of this article.

Dimensional stability is most easily evaluated using the water soaking method,[3] in which measured results are expressed as antishrink (antiswell) efficiency (ASE), as determined from eqs. (2) and (3).

$$S = (V_2 - V_1)/V_1 \times 100 \qquad (2)$$

where S = volumetric swelling coefficient, V_1 = volume of sample before water soaking test, and V_2 = sample volume after water soaking test. Thus,

$$\text{ASE} = (S_1 - S_2)/S_1 \times 100 \qquad (3)$$

where S_1 = volumetric swelling coefficient for untreated wood and S_2 = volumetric swelling coefficient for treated wood. Because the density of wood has a major effect on the amount of swelling, which occurs from water uptake, the test results are most accurate and precise when the untreated control sample has the same density (in the dry state) as the initial density of the WPC (wood density before treatment). As seen in Figure 1 for untreated wood (upper plot), the volumetric swelling increases with increasing density. This is reasonable, since an increase in wood density means an increase in the total amount of wood cell wall material for water to enter.

We see the opposite effect for weight increase vs. density (Fig. 1, lower plot); the lower the density of the wood, the greater weight of water it is capable of holding. This is due to the fact that a greater percentage of the total volume of wood is empty space (lumens), which water can enter through capillary action and strong surface attraction. The rate and amount of water uptake is greater at lower density (more lumens and pathways), but the amount of volume change is greater at higher density, since there is more structural material to absorb water with molecular and/or microscopic expansion.

Key goals for WPCs are to protect cell walls from water uptake (providing dimensional stability) and to slow or stop water imbibition (water incorporation into open lumens). The former is best obtained when cell wall properties are modified, that is, when the monomer penetrates the cell wall and the polymer that then forms interacts so strongly with the swellable components that interaction with water is no longer favorable or possible. There are almost always changes in other physical properties, caused by such *in situ* polymer reinforcement, and these changes are discussed below, with examples taken from our published work on EHMA-impregnated samples[4] and from the following article in this issue. See the former[4] for typical impregnation conditions, cure procedures, and sample loadings.

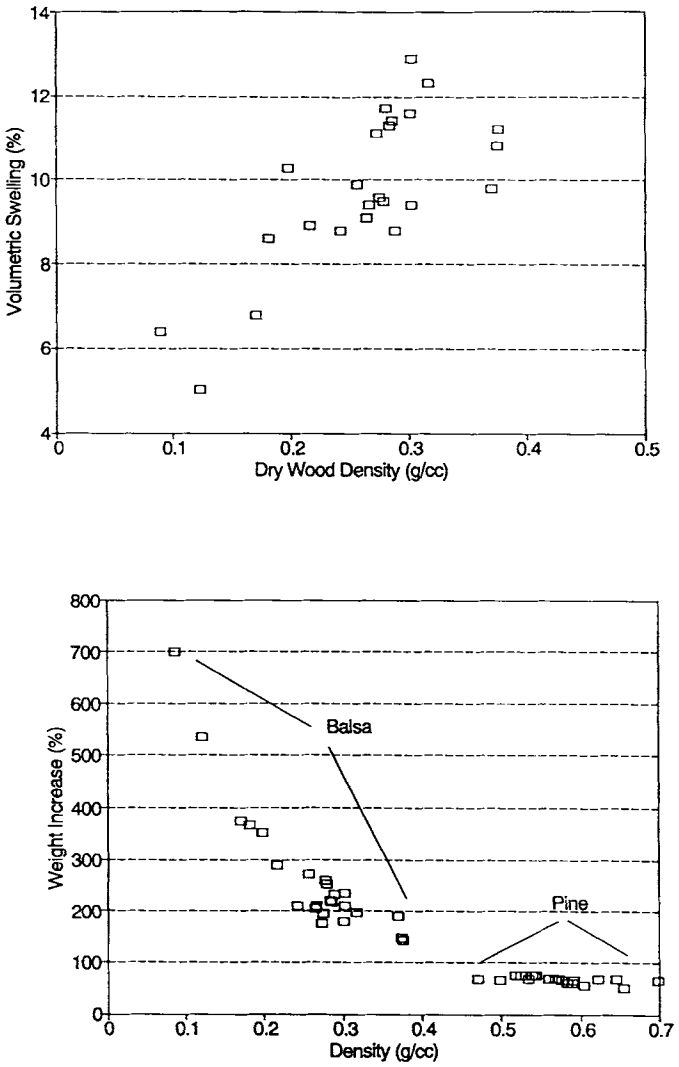

Figure 1 Effect of untreated wood density on volumetric swelling (upper plot) and weight gain (lower plot) due to water uptake. Samples were soaked in water at ambient temperature and pressure for 5 days.

MECHANICAL PROPERTIES TESTING

Wood is almost always anisotropic in its properties because of how it grows, combined with how nature equips it to support itself and resist deformation. Most mechanical properties of wood are, therefore, much greater along the grain than tangential to the grain and the measurement of mechanical properties must take into account grain orientation.

Dynamic Mechanical Thermal Analysis

The viscoelastic properties of wood and WPCs can be investigated using dynamic mechanical thermal analysis (DMTA). Dynamic mechanical tests involve applying a small stress in a time-varying sinusoidal or periodic manner. Thus, a storage modulus can be determined along with a phase angle or damping term δ. DMTA has been used to characterize the supermolecular structure of the wood cell wall via creep experiments.[5–7] Stress relaxation of wood has also been evaluated using DMTA; for example, the kinetics of the stress relaxation process in Scots pine veneer was investigated with regard to the initial effective stress.[8] We have found that DMTA is a particularly useful analytical method for WPCs because it is nondestructive, allowing the same test specimen to be analyzed before and after treatment. The effectiveness of the treatment can be determined with more validity because sample variability is minimized. Results of this nondestructive test should be used in conjunction with other

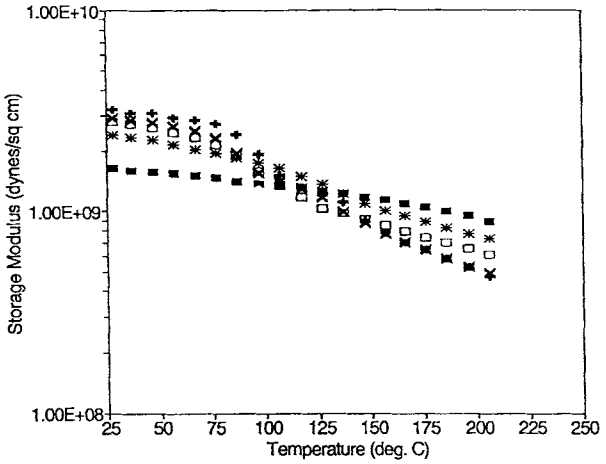

Figure 2 Dynamic mechanical analysis spectra of balsa WPCs made by impregnation with (*) EHMA only, (□) 3:1 EHMA-styrene, (×) 1 : 1 EHMA-styrene, (+) styrene only, and (■) control (no monomers).

methods (as shown below), involving alternative nondestructive measurements or catastrophic sample failure.

Dynamic mechanical analysis was used in our lab to determine the improvement in mechanical properties of the WPCs over those of untreated wood. For this particular test, the same sample was analyzed before and after treatment to eliminate sample variation effects. The DMA traces in Figure 2 indicate that the ambient temperature storage modulus increased as the styrene content (in mixtures of styrene with EHMA) increased; the greatest improvement was achieved using pure styrene. Based on the results discussed so far, it seemed reasonable to test the postulate that the most favorable *combination* of properties would be attained using EHMA (to provide dimensional stability) as a comonomer with styrene (or similar vinyl monomers) in WPC formation. The following article in this issue describes the results with balsa wood.

Buckled Plate Test

The buckled plate test is a destructive method, designed primarily for small rectangular-shaped samples. It is an excellent method for measuring interfacial adhesion in composites.[9] The test is performed on a tensile testing instrument and involves placing the sample upright between two compression platens and compressing the sample to failure by "buckling." The shape of the sample leads to a specific, well-defined mode of failure that can be enhanced by notching the sample. The slope of the stress–strain plot, and the amount of force necessary to fracture the sample, are used to calculate the compression modulus and strength, while fracture toughness is determined from the total energy required to break the sample. A major advantage of this test is that there are no gripping problems (sample crushing and/or slippage), as there are with conventional tensile testing.

As mentioned previously, there is a strong dependence of modulus and strength on density for whole wood. Figure 3 (lower plot) shows that the fairly linear relationship obtained appears to be independent of the two wood species (untreated samples). However, the compression moduli show a much better correlation at lower densities (balsa wood) than at higher densities (pine wood). This suggests that the higher the wood density, the greater the probability of having a softer region or a major defect leading to failure. In other words, the greater the percentage of cell wall in a given volume, the greater the chance of a structural defect or major sample variation. Thus, the upper edge of the data envelope represents the actual property relationship, with most deviations lying below this line due to imperfections and defects. For the treated balsa (Fig. 3, upper plot) the scatter is even greater and little correlation is evident. This may be due to the variation in starting wood property, combined with differences in sample treatments (a wide variety of conditions and impregnation materials were used). This again suggests that defects limit the potential physical property improvements that are expected for most impregnation processes.

For balsa wood, both wood compression modulus and toughness are related to specific gravity in the same general way, as illustrated in Figure 4. The two plots give the modulus and toughness values for the same untreated balsa samples, and they are almost identical in overall shape. This is reasonable, since modulus is related to sample stiffness, while toughness is related to the overall strength of the wood, and both are dependent on the amount of cell wall material per unit volume of wood, which is directly proportional to density.

Three-Point Bend Test

The three-point bend test, like the buckled plate test, is performed on a tensile testing instrument in the compression mode. This test is carried out by placing a specimen on two supports (one at each end) and by pressing on the specimen midway between the supports. The force necessary to bend or flex the specimen is used to calculate the flexural

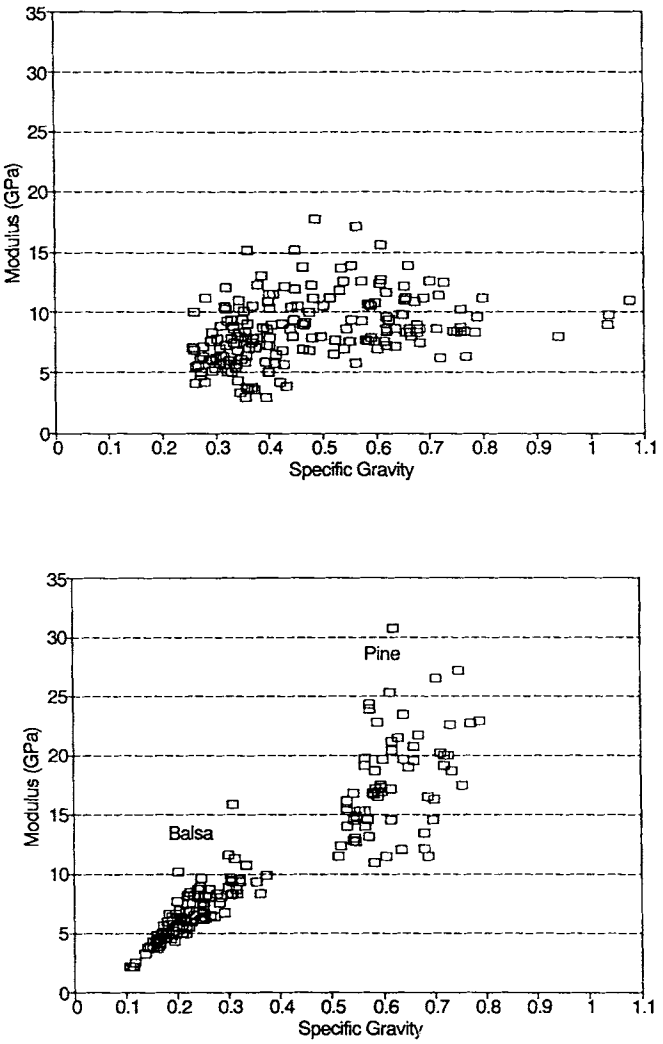

Figure 3 Sample modulus, plotted as a function of specific gravity for untreated balsa and pine (lower plot) and balsa WPCs (upper plot).

modulus. The flexural modulus is dependent on a material's tensile and compressive strength, since the test specimen is in compression on one side and in tension on the other. The flexural moduli of untreated balsa and Southern pine were plotted as a function of specimen density (Fig. 5). As with modulus and toughness measured by the buckled plate test, there is a clear dependence of flexural modulus on density. Again, at higher densities, the correlation is not as good as at lower densities, presumedly due to increased imperfections and defect concentrations.

Surface Hardness Test

Surface hardness is a material's resistance to indentation or marring. One of the most common test methods for plastics is the Rockwell hardness test.[10] This test measures the net increase in depth impression of a small steel ball, as the load on an indentor is increased from a fixed minor load to a major load and then is returned to the minor load. The standard hardness test for wood material is similar to the Rockwell hardness method and is carried out by measuring the load required to imbed a 1.128 cm steel ball, one-half its diameter, into the wood.[11] The test method we have developed is a modification of these two methods and was executed on an MTS 810 materials testing system. The test is best used to compare WPCs with control samples in order to determine the effect of treatment on surface hardness. A 3/16" diameter steel ball is used, and the amount of force required to imbed the ball to a depth of 0.5 mm is measured. The force is di-

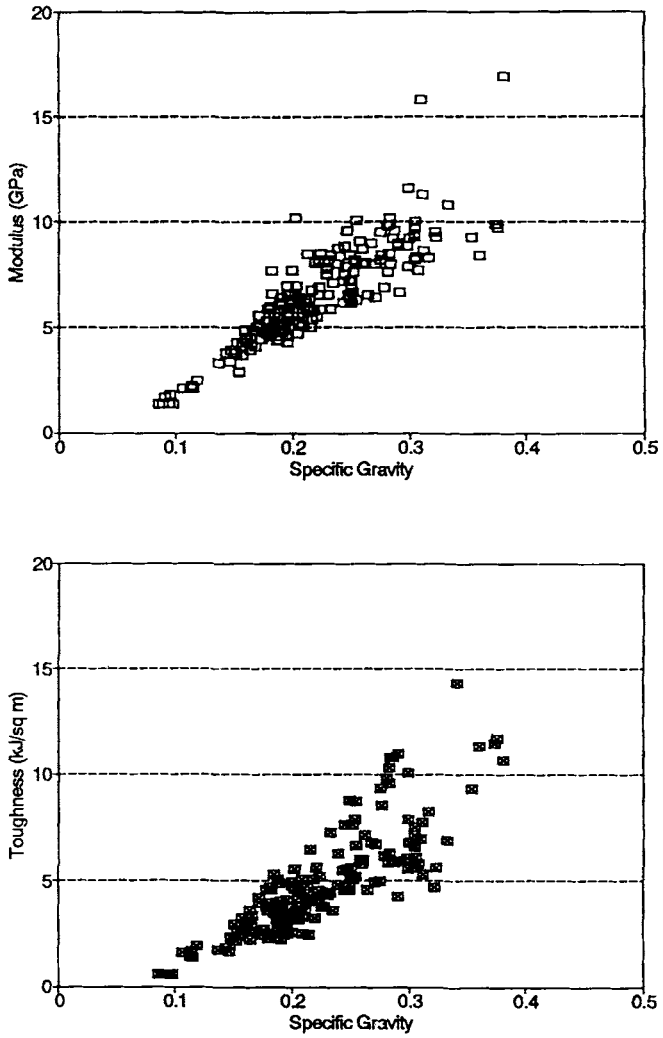

Figure 4 Sample toughness (lower plot) and modulus (upper plot) from buckled plate test, plotted as a function of sample specific gravity (density).

rectly proportional to the surface hardness, and the values measured, plus the change in measured hardness, are excellent indicators of property improvement.

As shown in Figure 6, wood density has a major effect on surface hardness. It also is clear that an increase in density, due to polymer incorporation, has at least as great an effect on the surface hardness as does the increase in density of untreated wood (due to increased concentrations of cell wall components). This seems reasonable, since lignocellulosic material is inherently not as hard as acrylic and styrenic polymers.

Table I summarizes the results of the surface hardness analyses for balsa and pine WPCs. Excellent improvement in surface hardness was demonstrated by each type of treatment listed, with increases ranging from 550% to 1435%. It is obvious that the increase in surface hardness is dependent on the amount of polymer in the composite, as illustrated in Figure 7. It should be mentioned that surface hardness does not depend as much on cell wall modification as on lumen filling; thus, it is easy to obtain significant improvement in hardness with little increase in dimensional stability or modulus, toughness, and strength. This lack of correlation was one of the major pitfalls of early work on WPCs, when it was often assumed that measurement of surface hardness alone was sufficient characterization.

Compressive Strength

The compressive strength of wood is also related to grain direction and direction of applied force. For compression in the direction parallel to the grain,

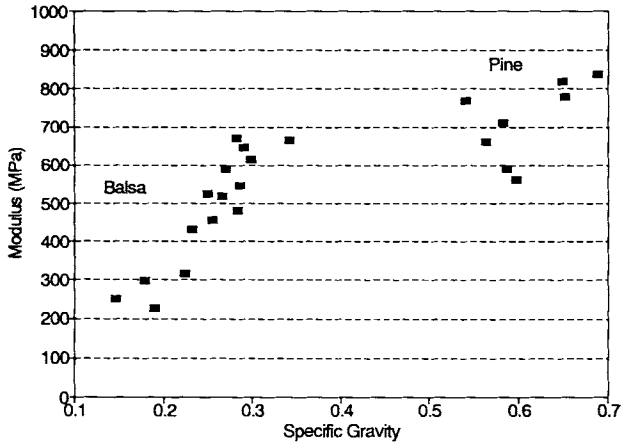

Figure 5 Flexural modulus from 3-point bending test, plotted as a function of specific gravity for untreated balsa and pine.

failure is initiated by a collapse of the submicroscopic structure in the cell wall. Folding of microfibrils occurs, which can be seen as diagonal lines on the cell wall using special microscopic techniques.[12] As the stresses increase, further failure is seen on a larger scale as crumpling of the wood cells into S-shapes, which eventually form wrinkles that are visible to the naked eye.

Compressive failure, perpendicular to the grain, occurs by collapse of the wood cells through flattening. This flattening can continue over large deformations without any clearly defined maximum load until nearly all the cells have collapsed and there is a large increase in stress. While initial strength values are much lower in this direction than in the parallel direction, perpendicular compression can actually lead to large increases in parallel properties, since little destruction of the fibers, cellulose crystallites, and other cell wall components occurs. This type of "densification" has been used as a method of wood property improvement, especially in conjunction with plasticization by heat or added water, solvent, or ammonia.

The results of compressive strength measurements for untreated balsa, aspen, pine, and oak are shown in Figure 8. The samples were $\frac{1}{4}$ in. cubes, which were compressed parallel to the grain. Again, there is a strong dependence of compressive strength on wood density, since the applied load is carried entirely by the cell wall material. The effect of increased moisture content is also seen in the plot. The plasticizing ability of water reduces compressive strength, and this effect seems to be more dramatic for wood of higher density.

ENVIRONMENTAL SCANNING ELECTRON MICROSCOPY

Conventional SEM requires high vacuum, dry specimens, and, usually, electrically conductive sur-

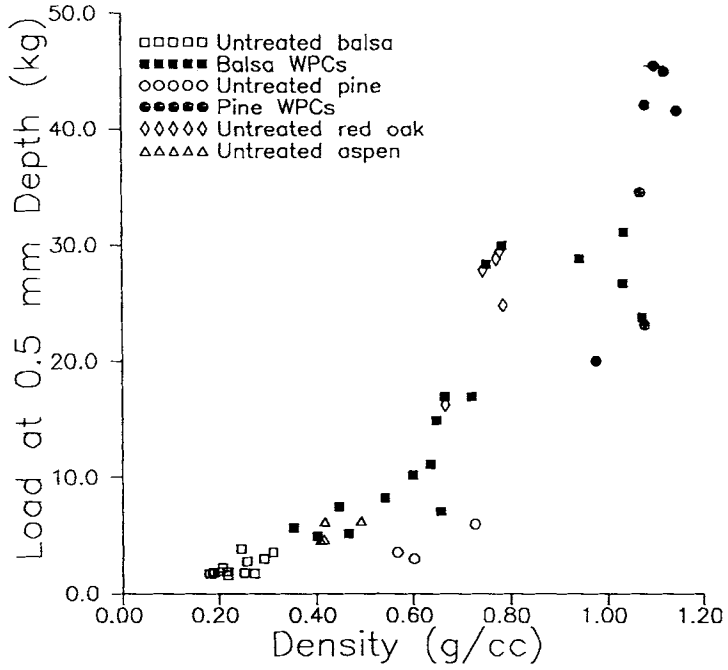

Figure 6 Surface hardness of various WPCs and untreated wood from indentation test, plotted as a function of wood density.

Table I Results of Surface Hardness Analyses for Balsa and Pine WPCs[a]

Wood/Treatment	Avg. Density (g/cm^3)	Avg. Weight Gain (%)	Avg. % Surface Hardness Increase
Pine/MHMA	1.1	81	552
Pine/ASM	1.1	94	614
Balsa/ASM	0.9	399	1435
Balsa/1 : 9 EHMA–ST	0.7	247	1043

[a] Listed are treated sample densities, average weight gains from impregnation, and measured increase in surface hardness (specimens indented with a $\frac{3}{16}$ in. steel ball at a test rate of 2 mm/min). MHMA and EHMA are the methyl and ethyl esters of α-hydroxymethylacrylate; ST is styrene and ASM is *p*-acetoxystyrene.

faces.[13] Coating the surface of nonconductive specimens (most polymers) with a conducting material, such as gold or carbon, has been necessary. This has precluded the viewing of wet or oily materials. Within the last decade, the environmental SEM (or ESEM) has been developed.[14,15] This instrument allows wet, oily, and electrically nonconductive specimens to be observed without special preparation and at relatively high pressures ($\sim$ 20 torr). The electron gun (which still requires high vacuum), the electron beam column, and the specimen chamber, are maintained at different pressures through the use of differential pumping.[16] A series of chambers along the beam path, each maintained at its own pressure, is linked by apertures. Vacuum pumps maintain the pressure gradients accurately, thus permitting the electron beam to pass from a high vacuum environment to the high pressure environment of the specimen. Figure 9 shows a schematic illustration of the ESEM.

A new type of detector has also been developed, which makes SEM imaging possible in the presence of gases, such as water vapor, oxygen, argon, and methane. The mechanism of detection and imaging will not be discussed here and the reader is referred to a detailed literature description.[17] Initial applications of the ESEM have included dynamic studies of crystal growth and direct observation of liquid transport in wet samples.[18–20]

The ESEM has proven useful for investigating wood–polymer interactions at fracture surfaces and polymer distribution in WPCs since surface modification (coating) that could block visualization and EDAX (energy dispersive analysis of x-rays; see below) is not required. Figure 10 is a SEM micrograph of a fractured balsa WPC, containing *p*-acetoxystyrene homopolymer (see the following article for additional details). It is evident that there is no adhesion of polymer to the cell walls, since the polymer surfaces are smooth and there is no indication of

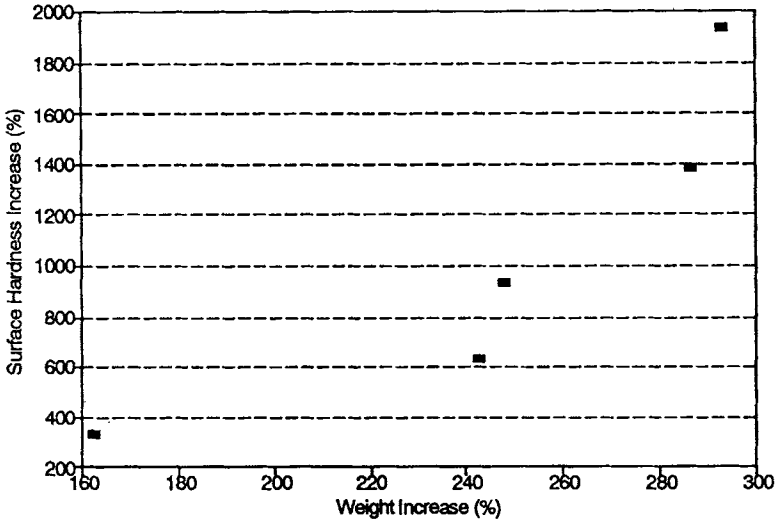

Figure 7 Improvement in surface hardness of balsa WPCs as a function of weight gain due to monomer uptake. Samples were impregnated with 1:9 EHMA-styrene.

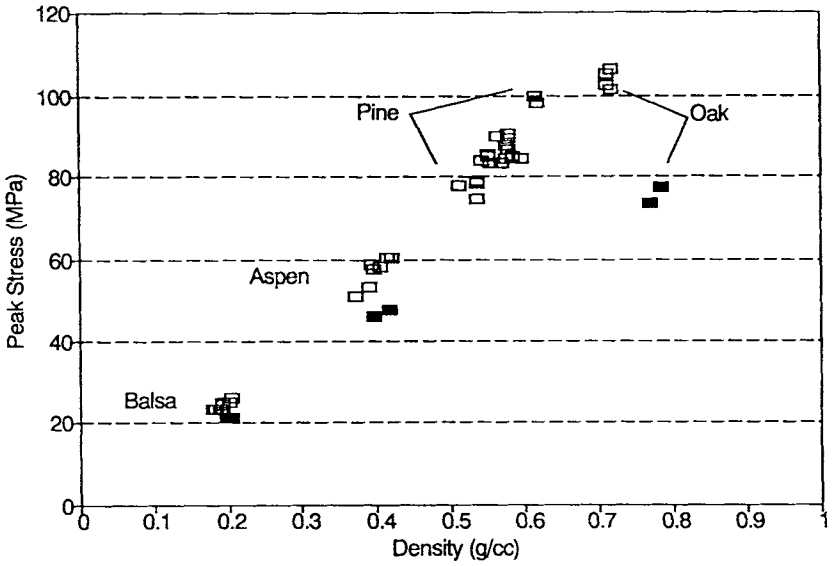

Figure 8 Compressive strength of untreated wood samples plotted as a function of density. (□) oven-dried samples, (■) samples containing ~ 8% moisture.

cellulose fibers adhering to the polymer. In contrast, good polymer–cell wall interaction is demonstrated in the balsa WPCs containing poly[ethyl α-(hydroxymethyl)acrylate] (Fig. 11). The intimate association between this polymer and the wood components is made evident by the presence of delaminated cellulose fibers that remained attached to the wood cell walls after fracture. The ESEM, then, can allows observation of the monomer-impregnated samples directly and after cure to WPCs to yield information on the interaction of the polymer formed with the wood components.

ENERGY DISPERSIVE ANALYSIS OF X-RAYS (EDAX)

Elemental composition can be determined using energy dispersive analysis of x-rays (EDAX). An energy dispersive x-ray analyzer, attached to an ESEM (or SEM), works on the principle that, when an electron beam of sufficient energy bombards a specimen, x-rays, characteristic of each element present, are emitted. From their energy and intensity, the atomic number and relative concentration of a particular element can be determined. The x-ray spectrum, shown in Figure 12, confirms the presence of polymer within the wood cell walls of a balsa WPC, containing a 1 : 1 copolymer of ethyl α-(hydroxymethyl)acrylate (EHMA) and ethyl α-(chloromethyl)acrylate (ECMA). A comonomer mixture, containing ECMA, was used for impregnation because it was rationalized that ECMA would diffuse along with EHMA into the cell walls (although less efficiently), and chlorine in the obtained copolymer

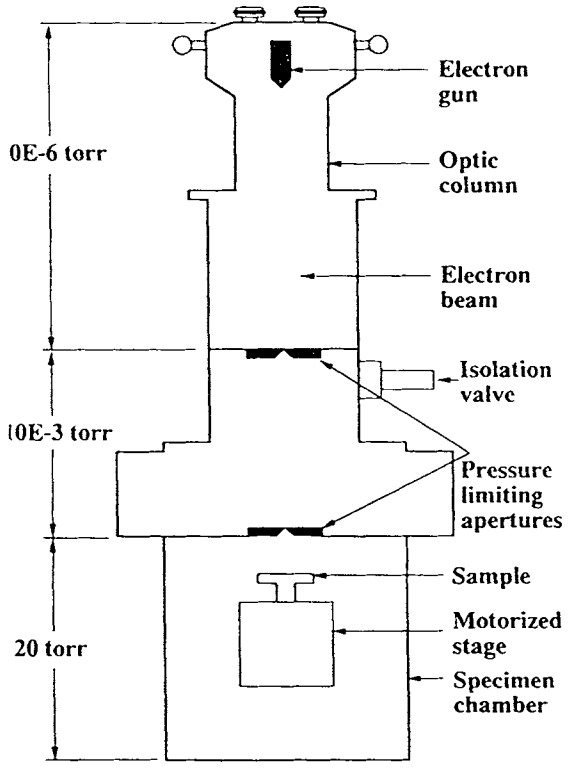

Figure 9 Schematic of the environmental scanning electron microscope.[18]

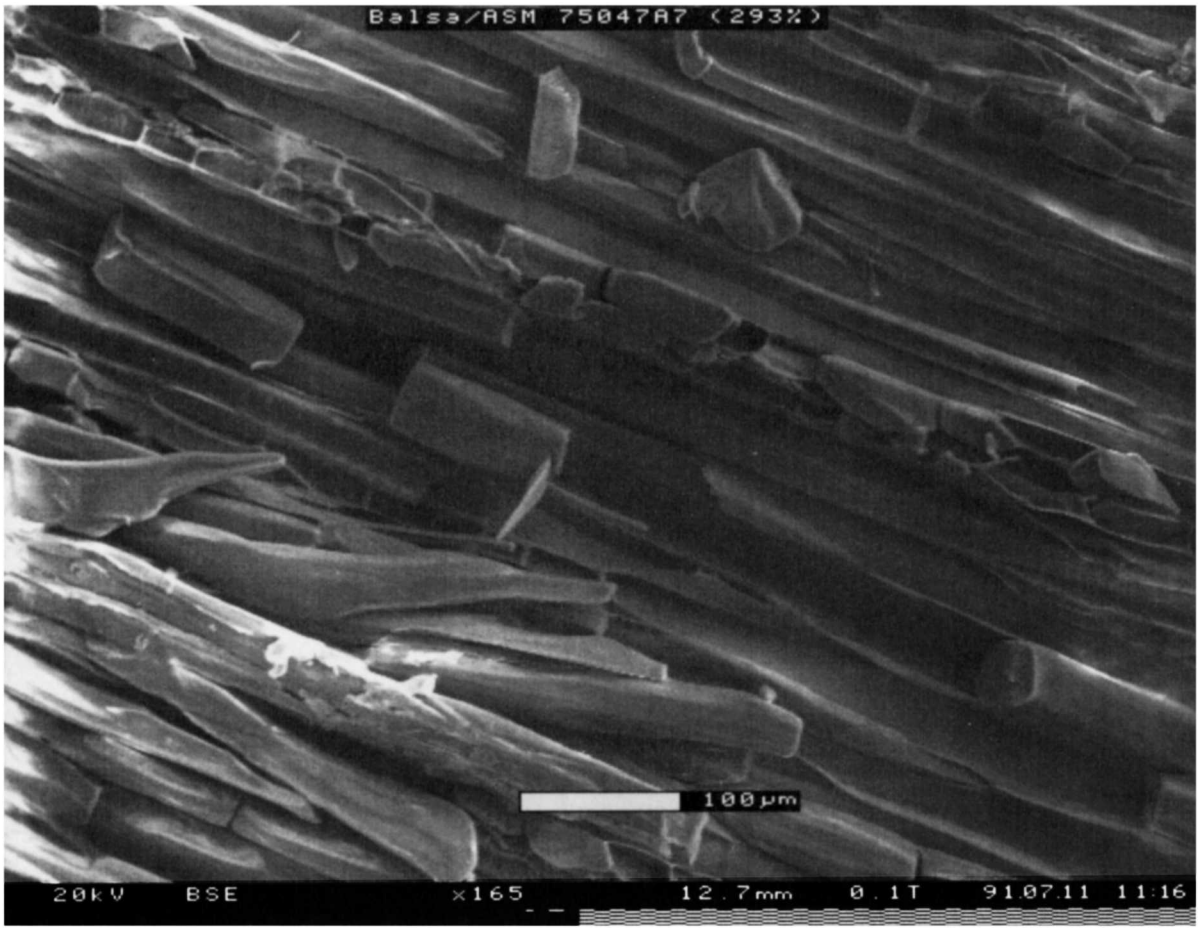

Figure 10 SEM micrograph of a split radial surface of a balsa/*p*-acetoxystyrene WPC.

would be easily detected by x-ray analysis. The area of the WPC analyzed is indicated by the crosshairs seen on the micrograph above the spectrum. This area was totally within a section of a wood cell wall of the fracture surface of a broken sample. The large K_α peak for chlorine verifies that the ECMA-containing polymer is *inside* the cell wall. This type of analysis is particularly useful in determining the depth of penetration of a chemical used for wood modification and to ascertain if the chemical is homogeneously distributed throughout the wood.

SOLID-STATE ^{13}C NMR SPECTROSCOPY

High resolution (solution) NMR spectroscopy is a very powerful technique for polymer analysis. It has been used to measure and to characterize polymer tacticity, helicity, mol wt, composition, comonomer sequence, diffusion coefficient, and propagation mechanism.[21] Solid-state ^{13}C NMR spectroscopy, using cross-polarization and magic angle spinning (CP/MAS), is especially useful for characterizing wood and WPCs, since detailed information can be obtained on solid, as-obtained samples. Such information may include composition, glass transition temperature, melting transitions, percent crystallinity, and number and type of crystalline phases.[22–25] In the particular case of cellulose, spectra demonstrating qualitative information have been described by several groups,[26,27] while a method for quantitative determination of cellulose crystallinity has recently been reported.[28] In general, solid state NMR involves proton–carbon cross polarization[29] to enhance the ^{13}C signal, high power decoupling[30] to eliminate dipolar line-broadening due to protons, and spinning of the sample about the magic angle of 54.74°, with respect to the static field,[31] to reduce chemical shift anisotropy effects.

A spectrum of Southern pine wood (Fig. 13) was obtained using CP/MAS in a Bruker MSL 200 spectrometer operating at a frequency of 50.32 MHz

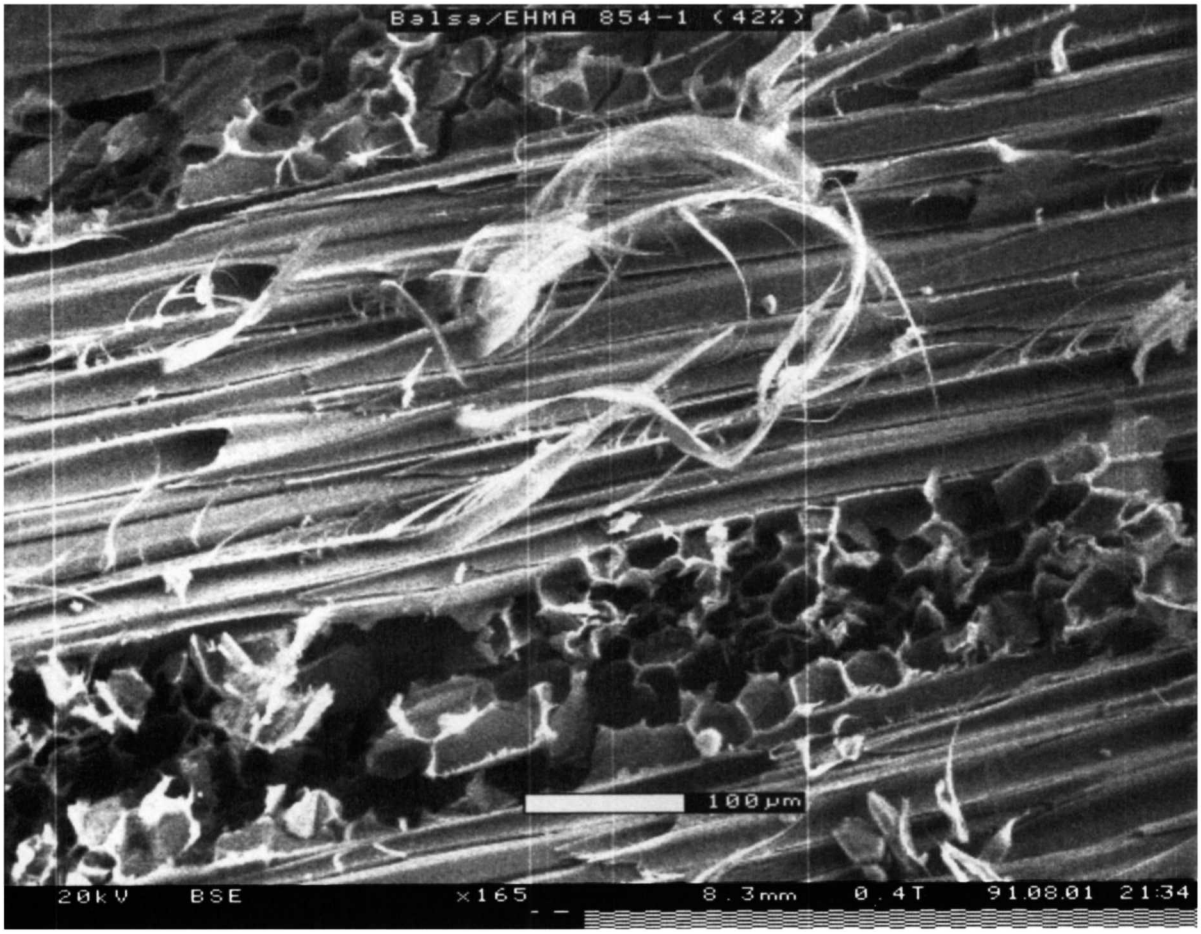

Figure 11 SEM micrograph of a split radial surface of a balsa/EHMA WPC.

for carbon. The peaks in the spectral region, from 160 ppm to 110 ppm, are due to the aromatic ring carbons of lignin, while those between ~160 ppm and ~143 ppm are assigned to oxygen-substituted aromatic carbons.[32] The signals, due to the lignin propyl carbons, overlap with signals due to the carbohydrate components of wood, and are not resolved. The peak at 56 ppm corresponds to lignin methoxy carbons ($Ar-OCH_3$), and the peaks at 122 and 135 ppm correspond to unsubstituted and alkylated aromatic carbons, respectively.[33] The acetyl groups from hemicellulose components yield peaks at 21 ppm (methyls) and 172 ppm (carbonyls).[34] The single peak at 105 ppm is assigned to the C-1 carbon of the cellulose anhydroglucose repeat unit (Fig. 13), while the signals at 89 and 84 ppm correspond, respectively, to cellulose carbon C-4 units in crystalline and noncrystalline domains.[28] The peaks at 66 ppm and 63 ppm are due to the C-6 carbon of cellulose. The somewhat broad, high-field shoulders, on the cellulose C-4 and C-6 signals, correspond to amorphous cellulose regions.[26] The cluster of resonances from 70 to 81 ppm is assigned to C-2, C-3, and C-5 cellulose carbons. Thus, chemical shift data allow qualitative and quantitative identification of the three major components of wood, plus determination of the cellulose crystallinity.

Proton Spin–Lattice Relaxation

After the magnetization vector, due to the alignment of nuclei, has been perturbed by the application of a pulse, it begins to relax back towards its equilibrium value by two processes, known as spin–spin and spin–lattice relaxation. Spin–lattice (or longitudinal) relaxation is brought about by the interaction of the spin with fluctuating magnetic fields, produced by random motions of neighboring nuclei. There are a number of interactions that can contribute to spin–lattice relaxation in a molecule. These processes include magnetic dipole–dipole, electric quadrupole, chemical shift anisotropy, sca-

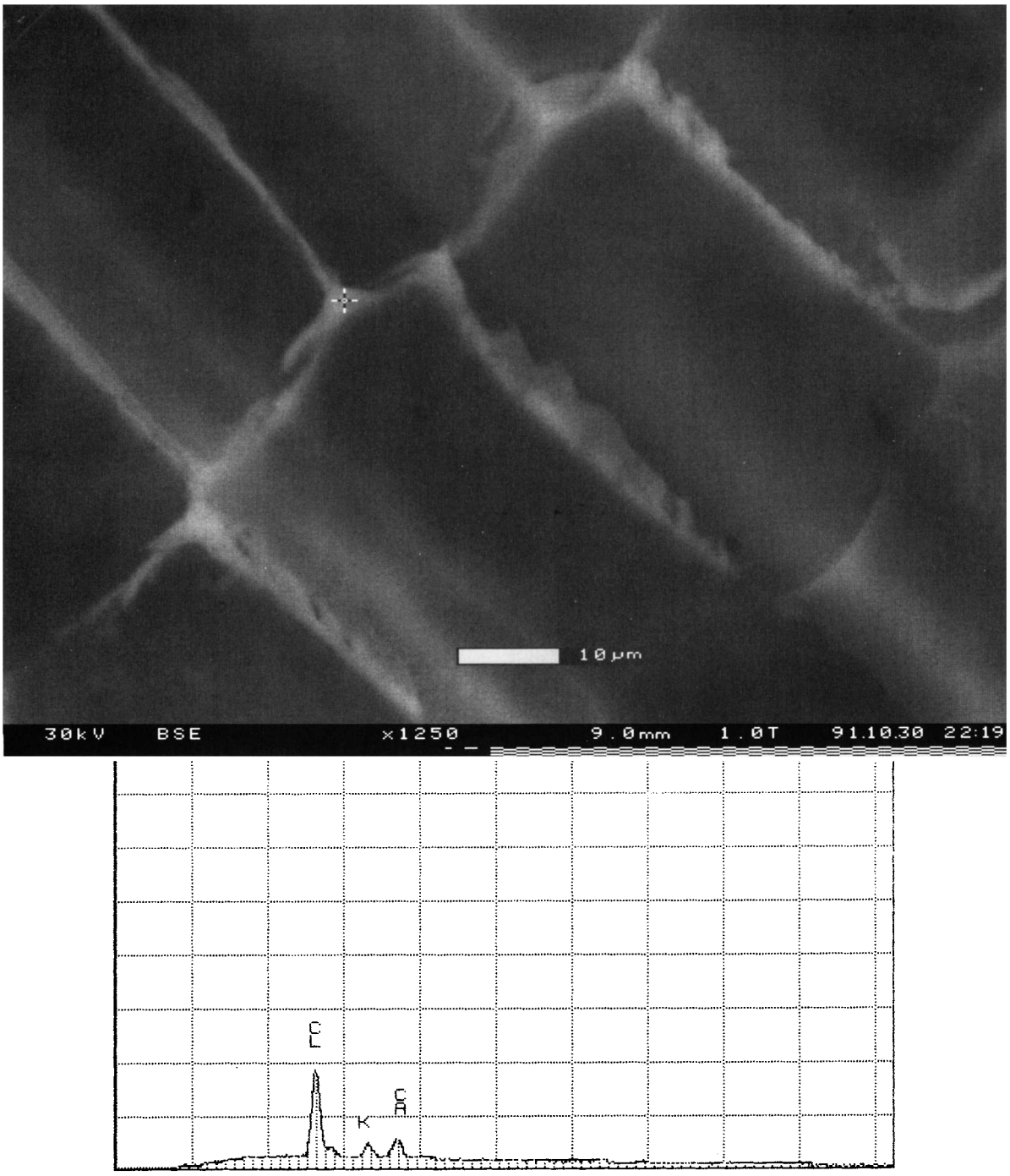

Figure 12 SEM micrograph (above) of a balsa WPC containing 1 : 1 EHMA–ECMA copolymer and EDAX spectrum (below).

lar-coupling, and spin-rotation.[35] Proton spin–lattice relaxation data have been used extensively for evaluating the miscibility of polymer blends.[36,37] Depending on the polymer peak chosen, the nature of the proton spin–lattice relaxation process in the immediate vicinity of a given blend component can be studied and compared to the relaxation behavior of the pure polymers. If the proton spin system is tightly coupled (good blend), the relaxation times should be independent of the carbon peak used to monitor signal decay.[38] Wood is an example of a natural polymer blend.

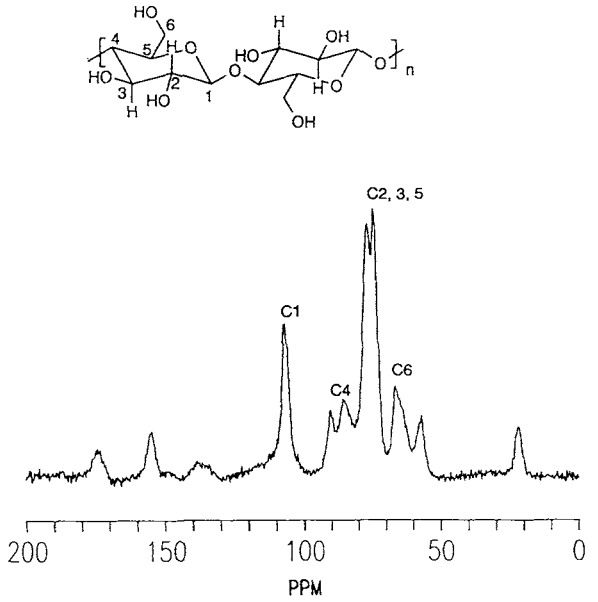

Figure 13 Solid-state ^{13}C NMR spectrum of Southern pine wood and structure of cellulose repeat unit.

Proton $T_{1\rho}$ relaxation times are spin–lattice relaxation times, measured with respect to the sample rotating frame, and are useful for blend analysis.[39] Values given here were obtained for untreated balsa wood, poly(EHMA), and a balsa WPC-containing poly(EHMA). Experiments were performed on a Bruker MSL 200 at a frequency of 50.32 MHz for carbon, with spinning rates of 4 kHz. The results of applying the proton $T_{1\rho}$ measurements indirectly, via ^{13}C CP/MAS for balsa/EHMA WPC, are presented in Figure 14. The pulse delay times ranged from 1 ms to 20 ms. The proton $T_{1\rho}$ relaxation times were obtained from a semilogarithmic plot of the intensity vs. delay time used in the cross-polarization experiment,[38] using the equation:

$$I_t = I_0 \exp(-\tau/T_{1\rho}), \qquad (1)$$

with I_t = peak intensity for each pulse delay time, I_0 = peak intensity for the longest delay time, τ = pulse delay, and $T_{1\rho}$ = relaxation time. Rearranging and taking the log gives:

$$\log I_t/I_0 = (-\tau/2.303)(1/T_{1\rho}), \qquad (2)$$

where the reciprocal of the slope is the relaxation time.

Representative semilogarithmic plots of delay times, as a function of resonance intensity, are displayed in Figure 15. The bottom trace is for one of the balsa wood peaks in the untreated sample, while the middle and upper traces are for the composite and pure EHMA polymer, respectively. Relaxation times were determined for three unique peaks of each of the WPC components, with the results shown in Table II. It is evident that wood and poly(EHMA) each have tightly coupled proton spin systems, since the relaxation times for all peaks measured for each sample were basically the same (within experimental error). The proton $T_{1\rho}$ times for individual peaks of the composite are different from each other, however, since the composite is heterogeneous, containing separate domains consisting of wood and polymer. Peaks for the polymer component of the composite exhibited relaxation behavior, similar to the pure polymer sample (with the exception of the peak at 61.4 ppm), while the wood component peaks exhibited relaxation behavior that was similar to that of pure wood. The 61.4 ppm peak of the composite (middle trace in Fig. 15) displays a two-component relaxation process, which is different from the single component behavior of the peaks associated with only the wood or polymer segments. The first half of the plot has a slope that is similar to the slope of pure poly(EHMA), while the second-half slope corresponds to the slope of balsa wood. This two-component behavior is caused by the fact two peaks overlap in the WPC spectrum [the C6 carbon of

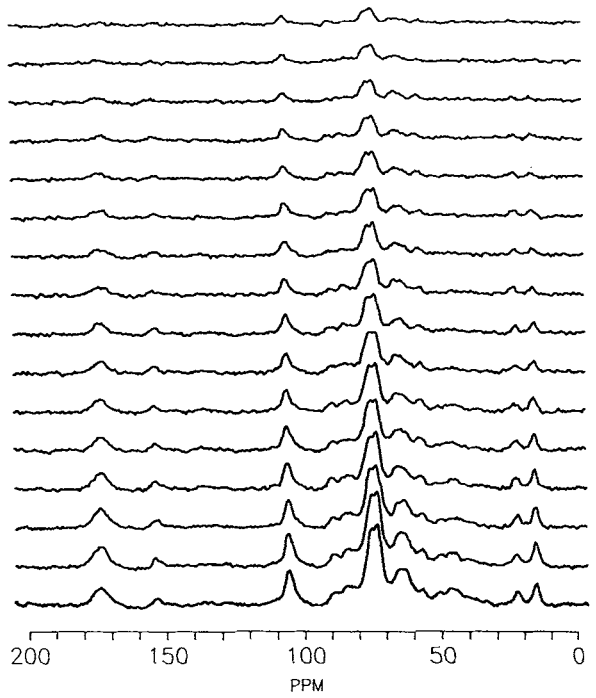

Figure 14 Solid-state ^{13}C NMR spectra of balsa/EHMA WPC used to determine ^{1}H $T_{1\rho}$ relaxation times. Delay times ranged from 1 msec (bottom) to 20 msec (top).

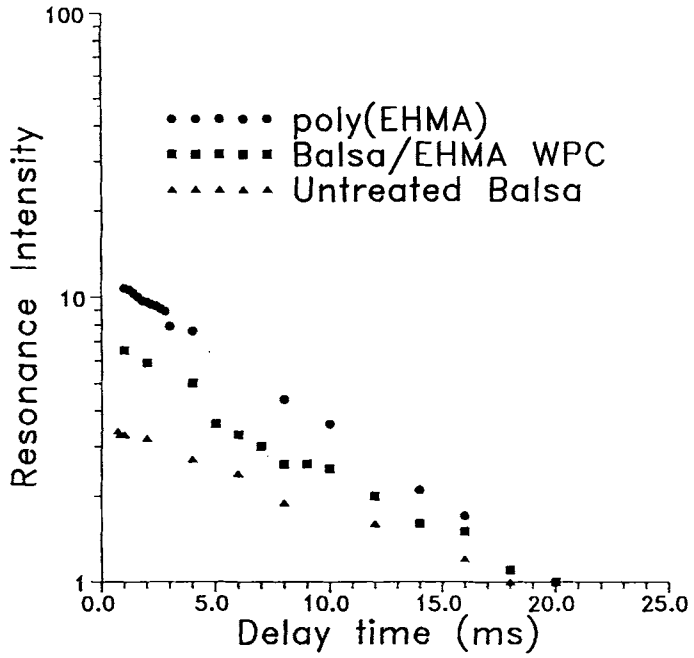

Figure 15 Semilogarithmic plot of the measured relative ^{13}C CP/MAS resonance intensity vs. delay time. The peaks chosen for plotting were at 61.4 ppm (poly-EHMA & composite) and 72.5 ppm (balsa wood).

cellulose and the hydroxymethyl carbon of poly(EHMA)] and additive relaxation behavior is observed, as expected, for nonaveraged environments.[39]

While these results illustrate the ability to differentiate readily the chemically distinct components or domains within a heterogeneous sample, sufficient peak sensitivity and resolution is not available to allow direct observation of the blendlike component at the interface or within the interphase between the separate phases. New techniques are under development that will allow this, however, and these will make solid-state NMR one of the most sensitive methods for qualitative and quantitative determination of composition and blend (WPC) component interaction.

Table II Proton $T_{1\rho}$ Relaxation Times for Peaks of Pure Poly(Ethyl α-hydroxymethylacrylate) (p-EHMA), Untreated Balsa Wood (Balsa), and Balsa Wood Impregnated With Poly(Ethyl α-hydroxymethylacrylate) (WPC)

	^1H $T_{1\rho}$ (ms)		
	p-EHMA	WPA	Balsa
C_1 (174.8 ppm)	7.7	6.8	—
C_2 (105.0 ppm)	—	11.9	12.8
C_3 (72.5 ppm)	—	11.4	12.4
C_4 (61.4 ppm)	8.0	7.3 & 11.7	—
C_5 (20.9 ppm)	—	12.1	13.5
C_6 (14.1 ppm)	8.1	5.8	—

This work was supported in part by a grant from the National Renewable Energy Laboratory, Golden, Colorado, through a contract from the Department of Energy, Energy Conservation and Utilization Technology/Biomass Materials Program. The Bruker MSL-200 NMR used in this project was obtained with a Department of Defense Instrumentation Grant through the Office of Naval Research.

REFERENCES

1. U. S. Department of Agriculture, Forest Service. *Wood Handbook: Wood as an Engineering Material,* USDA Agric. Handb., Washington, DC, 1955, p. 72.
2. A. J. Stamm, *Wood and Cellulose Science,* Ronald, New York, 1964.
3. R. M. Rowell and W. D. Ellis, *Wood and Fiber,* **10**(2), 104 (1979).
4. J. R. Wright and L. J. Mathias, *Polym. Engin. Sci.,* **32,** 370 (1992).
5. H. Schniewind, *Wood Sci. Tech.,* **2,** 188 (1968).
6. M. Mori, M. Norimoto, and T. Yamada, *Wood Res.,* **56,** 33 (1974).

7. W. E. Hillis and A. N. Rozsa, *Holzforschung,* **32,** 68 (1978).
8. D. G. Kubat, S. Samuelsson, and C. Klason, *J. Mater. Sci.,* **24,** 3541 (1989).
9. R. L. Brady, R. S. Porter, and J. A. Donovan, *J. Mater. Sci.,* **24,** 4138 (1989).
10. *American Society for Testing and Materials,* ASTM Stand. Desig. D 785-65 (reapproved 1970), Philadelphia, 1972.
11. *American Society for Testing and Materials,* ASTM Stand. Desig. D 143-52 (reapproved 1972), Philadelphia, 1972.
12. F. F. Wangaard, Ed., *Wood: Its Structure and Properties,* Pennsylvania State University, University Park, Pennsylvania, 1981.
13. R. B. Bolon, C. D. Robertson, and E. Lifshin, *Microbeam Analysis,* P. E. Russell, Ed., San Francisco Press, San Francisco, 1989.
14. G. D. Danilatos, *Scanning,* **7,** 26 (1985).
15. G. D. Danilatos, *Adv. Electronics and Electron Phys.,* **71,** 109 (1990).
16. K. Sujata and H. M. Jennings, *Mater. Res. Soc. Bull.,* **16,** 41 (1991).
17. G. D. Danilatos, *J. Microscopy,* **160,** 9 (1990).
18. E. Doehne and D. Stulik, *Mat. Res. Soc. Symp. Proc.,* **185,** 31 (1991).
19. E. Doehne and D. Stulik, *Scanning Microscopy,* **4,** 275 (1990).
20. G. D. Danilatos and J. V. Brancik, *Proc. of the 44th Annual Meeting of the Electron Microscopy Soc. of America,* G. W. Baily, Ed., San Francisco Press, San Francisco, 1986.
21. R. Ramharack, *Polymer News,* **13,** 174 (1988).
22. C. S. Yannoni, *Acc. Chem. Res.,* **15,** 201 (1982).
23. R. E. Wasylishen and C. A. Fyfe, *Ann. Rep. NMR Spectrosc.,* **12,** 1 (1982).
24. B. C. Gerstein, *Anal. Chem.,* **55,** 781A (1983).
25. B. C. Gerstein, *Anal. Chem.,* **55,** 899A (1983).
26. W. L. Earl and D. L. VanderHart, *J. Am. Chem. Soc.,* **102,** 3251 (1980).
27. R. H. Atalla, J. C. Gast, D. W. Sindorf, V. J. Bartuska, and G. E. Maciel, *J. Am. Chem. Soc.,* **102,** 3249 (1980).
28. R. H. Newman and J. A. Hemmingson, *Holzforschung,* **44,** 351 (1990).
29. S. R. Hartmann and E. L. Hahn, *Phys. Rev.,* **128,** 2042 (1962).
30. L. R. Sarles and R. M. Cotts, *Phys. Rev.,* **111,** 853 (1958).
31. E. R. Andrew, *Arch. Sci. (Geneva),* **12,** 103 (1959).
32. J. F. Haw, G. E. Maciel, and H. A. Schroeder, *Anal. Chem.,* **56,** 1323 (1984).
33. P. Tekely and M. R. Vignon, *J. Polym. Sci. Part C Polym. Let.,* **25,** 257 (1987).
34. B. L. Browning, *The Chemistry of Wood,* R. E. Krieger, Huntington, New York, 1975.
35. T. C. Farrar and E. D. Becker, *Pulse and Fourier Transform NMR: Introduction to Theory and Methods,* Academic, New York, 1971.
36. J. F. Parmer, L. C. Dickenson, J. C. W. Chien, and R. S. Porter, *Macromolecules,* **22,** 1078 (1989).
37. J.-F. Masson and R. St. J. Manley, *Macromolecules,* **24,** 6670 (1991).
38. C. A. Fyfe, *Solid State NMR for Chemists,* C. F. C. Press, Guelph, Ontario, Canada, 1983, p. 51.
39. J. Schaefer, E. O. Stejskal, and R. Buchdahl, *Macromolecules,* **10,** 384 (1977).

Received June 10, 1992
Accepted October 5, 1992